2023 SCEC progress report for Shaw

"Developing earthquake simulators for UCERF4"

Bruce E. Shaw, Columbia University

Lamont Doherty Earth Observatory, Palisades NY 10964, 845-359-2900, FAX: 845-365-8150, shaw@ldeo.columbia.edu

With support from this SCEC grant, progress on a number of fronts related to earthquake simulators and next generation hazard models has been made. One area of progress involves using simulators to improve understanding of scaling relations relevant for use in fault-based seismic hazard. A second area of progress is in using simulator events as a guide in helping improve rupture plausibility filters to better estimate fault connectivity and rupture sets for use in UCERF4 and the 2023 NSHM. In the last year, two papers have been published on these topics. All have relevance to NSHM efforts. The first one (*Milner, Shaw, and Field, 2022*) was published in the *Bulletin of the Seismological Society of America*. The second one (*Shaw, 2023*) was published in the *Bulletin of the Seismological Society of America*. Below, some results from these papers are presented.

Published paper using simulator to improve estimates of multifault ruptures

" Enumerating Plausible Multifault Ruptures in Complex Fault Systems with Physical Constraints", (*Milner, Shaw, and Field, 2022*)

We propose a new model for determining the set of plausible multifault ruptures in an interconnected fault system. We improve upon the rules used in the Third Uniform California Earthquake Rupture Forecast (UCERF3) to increase connectivity and the physical consistency of ruptures. We replace UCERF3's simple azimuth change rules with new Coulomb favorability metrics and increase the maximum jump distance to 15 km. Although the UCERF3 rules were appropriate for faults with similar rakes, the Coulomb calculations used here inherently encode preferred orientations between faults with different rakes. Our new rules are designed to be insensitive to discretization details and are generally more permissive than their UCERF3 counterparts; they allow more than twice the connectivity compared to UCERF3, yet heavily penalize long ruptures that take multiple improbable jumps. The set of all possible multifault ruptures in the California fault system is near-infinite, but our model produces a tractable set of 298,542 ruptures (a modest 18% increase over UCERF3, despite the greatly increased connectivity). Inclusion in the rupture set does not dictate that a rupture receives a significant rate in the final model; rupture rates are solely determined by data constraints used in the inversion. We describe the rupture building algorithm and its components in detail, and provide comparisons with ruptures generated by a physics-based multicycle earthquake simulator. We find that nearly twice as many ruptures generated by the simulator violate the UCERF3 rules than violate our proposed model.

In developing a new set of criteria to improve the rupture set feeding into rupture forecast inversions, we used a dialog with the simulator output to test the new Coulomb-based measures. Figure 1 illustrates this dialog. Figure 1a illustrates the Coulomb interactions between faults used as a physical basis for building plausible ruptures. Care was taken to develop a series of measures based on coulomb interactions which were robust and insensitive to discretizations. Figure 1b shows a comparison of distributions of rupture jump azimuths using the previous UCERF3 filter, the emergent RSQSim simulated ruptures, and the new UCERF4 filters. We see a much better agreement of the new filters with the simulated ruptures. Figure 1c shows a comparison of the rate of simulated ruptures failing the previous UCERF3 rupture filters as compared with the new UCERF4 filters. We see also most of the ruptures which do fail are based on one or two subsections on large ruptures failing, which also supports the new approach as these indicate ruptures attempting to take branches and then dying out. Again we see better agreement of the new UCERF4 filters with the simulated ruptures as compared with the old UCERF3 filters.

Published paper using simulator to improve scaling relations for use in fault-based seismic hazard

" Magnitude and Slip Scaling Relations for Fault Based Seismic Hazard" (*Shaw, 2023*)

Simulators were used as a guide to developing the recommended scaling relations in this paper. While ultimately the scaling relations and results in the paper came from existing scaling relations and statistical analysis of observational data, the simulators helped inform the recommendations. Below are cited results from the paper.

Scaling relations play an important role in fault-based seismic hazard estimates. Scaling relations impact estimates of the sizes and rate for a given fault area. Here we examine which relations are most useful for these estimate, and issues that arise. These include the depth of large event ruptures, transient deepening of seismicity following large events, difficulties in using classical continuum exponent fits, and the importance of large event asymptotics. A new analysis of land-based data calls into question non-specific exponent fitting, which is a standard practice. We show a dependence on the lower and upper cutoff magnitudes in the data in the best fitting slope parameter relating magnitude to log area with this approach. We show as well a dependence on assumed data uncertainties. These sensitivities make using this quite standard approach very problematic. Based on this evidence and other factors, we propose recommendations for minimal branch sets which preserve epistemic uncertainty for use in fault-based seismic hazard estimates.

In *Shaw* (2023) we have analyzed magnitude and slip scaling relations in the context of fault-based seismic hazard. This work aided the NSHM effort by providing scaling recommendations. It additionally produced a number of interesting results of relevance to hazard, including showing that the traditional method of *Wells and Coppersmith* (1994) is problematic, producing best fitting slopes in log-log space that depend on magnitude limits. Figure 2 illustrates some of this work.

Figure 3 illustrates fits of the recommended scaling relations compared with Magnitude-Area and Surface Slip-Length data.

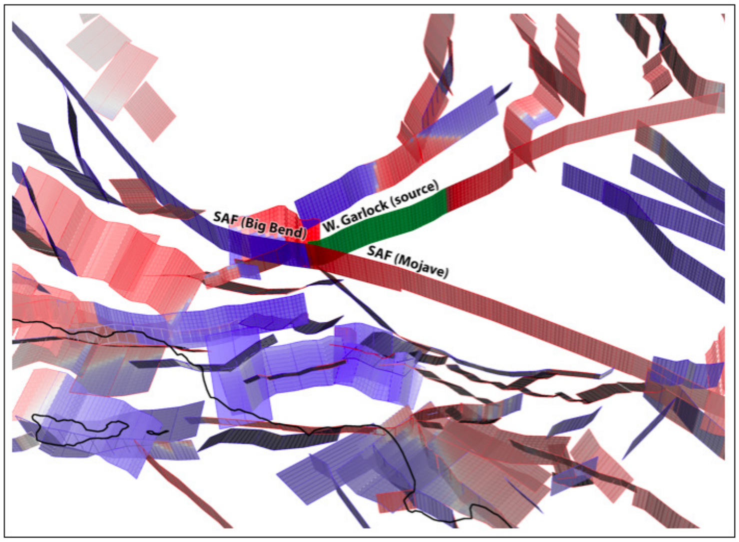

(a)

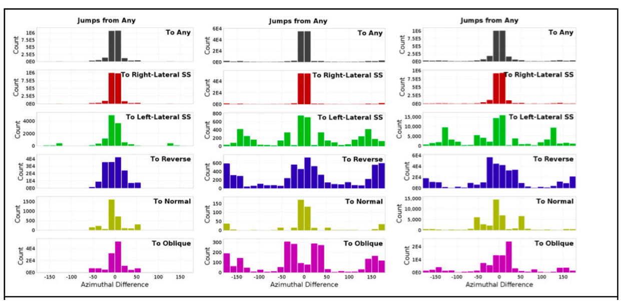

(b)

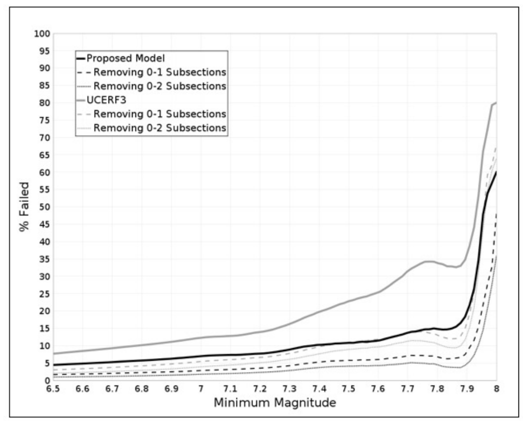

(c)

Figure 1: (a) Figure illustrating Coulomb interactions incorporated into measures used to select multifault ruptures. 3D view looking north of faults from the Third Uniform California Earthquake Rupture Forecast (UCERF3) model broken up into 2 km x 2 km patches for Coulomb calculations. Patches overlap slightly in order to fill the fault surfaces completely. In this example, eight subsections of the Garlock fault are used as sources (green) and Coulomb stress changes are computed to all other patches (with contributions summed across all source patches). Receiver patches are colored by their sign with darker colors indicating greater amplitude, and subsection outlines are colored by the sum across all receiver patches (red is positive, blue negative). This shows the Coulomb-preferred corupture direction of the left-lateral Garlock Fault connecting to the Mojave section of the right-lateral San Andreas Fault (SAF). Coastlines are overlaid in black. (b) Comparison of distributions of jump azimuths in previous UCERF3 filter, RSQSim simulated ruptures, and new UCERF4 filter. The new filters show improved match with simulated ruptures. Jump azimuth changes allowed, from left to right, in the UCERF3 model, the comparison Rate-State Earthquake Simulator (RSQSim) model, and the new model proposed here. Each differently-colored subplot (arranged in rows) corresponds to jumps from any type of fault to a fault of that type, e.g., the 3rd row from the top represents all azimuth changes at jumps either to, from, or between left-lateral strike-slip faults. (c) Comparison of fraction of RSQSim simulated ruptures failing UCERF3 filters compared with new UCERF4 filters. An improved match is seen with new filters. The rate at which ruptures from the RSQSim comparison model fail the plausibility filters used in UCERF3 (solid gray line) and proposed here (solid black line), as a function of magnitude. This excludes the minimum number of subsections per cluster filter, which is common to both models and was not intended to gauge rupture plausibility. Failure rates are also given for rupture subsets where up to one (dashed lines) and two (dotted lines) subsections are removed from an end of a participating fault section; this shows that the majority of failing ruptures are largely compatible except for one or two incompatible subsections. From (*Milner, Shaw, and Field, 2022*)

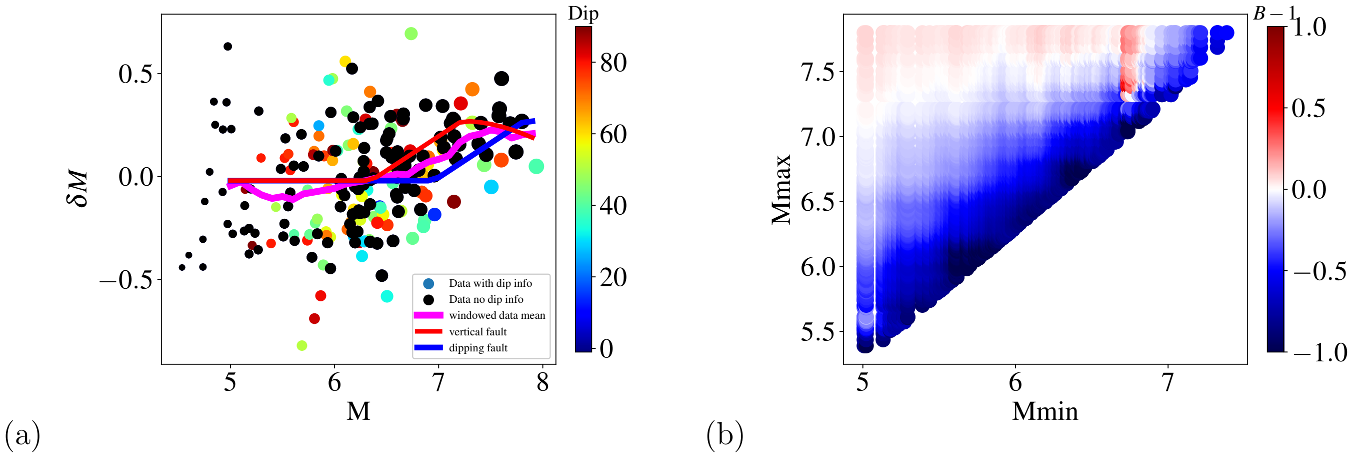

Figure 2: Aided NSHM effort through scaling relations study. (a) New refined approach subtracts off main trend and looks at deviations from that, plotting Magnitude residual $\delta\mathbf{M}{=}\mathbf{M} - \log_{10} A - 4.0$ versus magnitude. Color is dip (black color is no dip information). Magenta line is mean residual averaged over magnitudes within 0.3 magnitude units on either side. Free surface effects and finite seismogenic width effects can be seen in looking at the residuals plot. This causes curvature in the data, makes fitting a straight line to the data problematic. From *Shaw* (2023). b) Best fitting slope of line using *Wells and Coppersmith* (1994) method to (*Wells and Youngs*, 2015) data shows best fitting slope depends on lower and upper magnitude cutoffs $\mathbf{M}_{min}$ and $\mathbf{M}_{max}$. Difference from reference unity slope is plotted. From *Shaw* (2023)

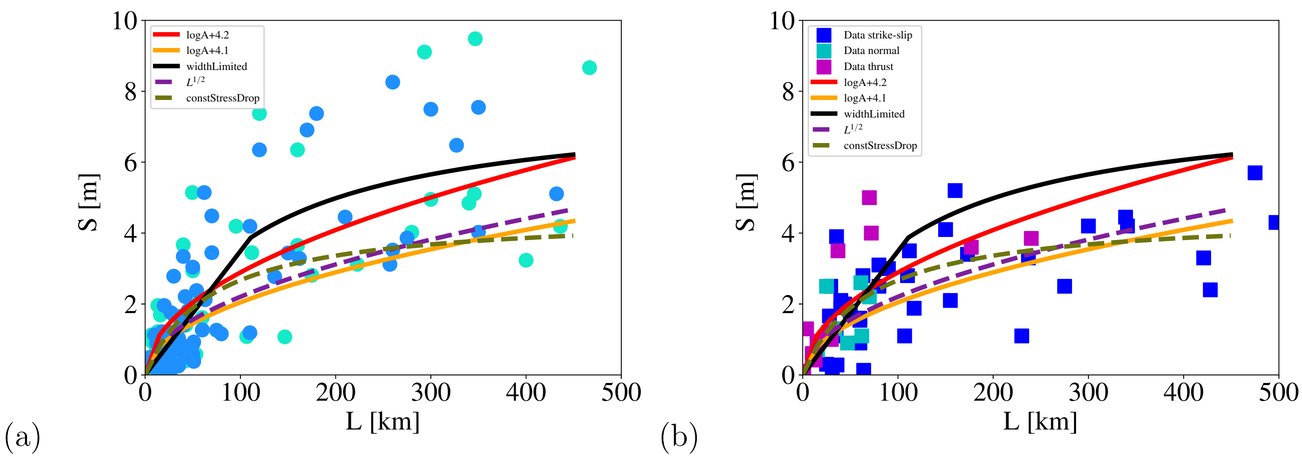

Figure 3: Slip length scaling relations for plate boundary events. Solid lines are implied slip-length scaling relations derived from Magnitude-Area scaling relations, and not rescaled to data, as in previous figure. Dashed lines are slip-length scaling relations derived from surface slip observations. (a) Data from magnitude area, with slip from moment divided by area and modulus. Blue points are data from (*WGCEP*, 2003). Light blue points are data from (*Hanks and Bakun*, 2008). Note the solid lines fit this data better than the dashed lines. (b) Data from surface slip measurements from *Biasi et al.* (2012) database. Blue squares are strike-slip events, cyan squares are normal events, magenta squares are thrust events. There is sufficient overlap between the different mechanisms that neglecting mechanism appears to be a not bad approximation and thus useful simplification. Note now the dashed lines fit this data better than the solid lines. Solid red line is implied slip-length from Ellsworth-B LogA scaling with $C = 4.2$ magnitude-area relation. Solid orange line is implied slip-length for LogA scaling with reduced $C = 4.1$ value. Solid black line is implied slip-length from widthLimited scaling (*Shaw*, 2009). Dashed purple line is $L^{1/2}$ scaling. Dashed dark green line is constant stress drop scaling for surface slip (*Shaw*, 2013). From (*Shaw*, 2023)

References

Biasi, G., T. Dawson, and R. Weldon, Preliminary event data for ucerf3, *private communication*, 2012.

Ellsworth, W. L., Magnitude and area data for strike slip earthquakes, *U.S. Geol. Surv. Open File Rep., 03-214 Appendix D*, 2003.

Hanks, T. C., and W. H. Bakun, M-log A observations of recent large earthquakes, *Bull. Seismol. Soc. Am.*, *98*, 490, 2008.

Milner, K. R., B. E. Shaw, and E. H. Field, Enumerating plausible multifault ruptures in complex fault systems with physical constraints, *Bull. Seismol. Soc. Am.*, *112*, doi: 10.1785/0120210322, 2022.

Shaw, B. E., Constant stress drop from small to great earthquakes in magnitude-area scaling, *Bull. Seismol. Soc. Am.*, *99*, 871, doi:10.1785/0120080006, 2009.

Shaw, B. E., Earthquake surface slip length data is fit by constant stress drop and is useful for seismic hazard analysis, *Bull. Seismol. Soc. Am.*, *103*, 876, doi:10.1785/0120110258, 2013.

Shaw, B. E., Magnitude and slip scaling relations for fault based seismic hazard, *Bull. Seismol. Soc. Am.*, doi: 10.1785/0120220144, 2023.

Stirling, M., T. Goded, K. Berryman, and N. Litchfield, Selection of Earthquake Scaling Relationships for Seismic-Hazard Analysis, *Bull. Seismol. Soc. Am.*, *103*(6), 2993–3011, doi:10.1785/0120130052, 2013.

Wells, D., and B. Youngs, Improved regression relations for earthquake source parameters, *Seismol. Soc. Annual Meeting*, p. Abstract, 2015.

Wells, D. L., and K. J. Coppersmith, New empirical relationships among magnitude, rupture length, rupture width, rupture area, and surface displacement, *Bull. Seismol. Soc. Am.*, *84*, 974, 1994.

WGCEP, Earthquake probabilities in the San Francisco Bay Region: 2002 to 2031, *U.S. Geol. Surv. Open File Rep., 03-214*, 2003.